

Article

Not peer-reviewed version

---

# Cytostatic Effects of Hydroalcoholic Extract of *Justicia spicigera* on LNCaP Prostate Cancer Cells: Cell Cycle Arrest and Apoptosis Induction

---

Ivette Bravo-Espinoza <sup>†</sup> , [Fabiola Hernández-Rosas](#) <sup>†</sup> , [María Elena Hernández-Aguilar](#) ,  
Marycarmen Godínez-Victoria , [Rodrigo Rafael Ramos-Hernández](#) , [Carlos Alberto López-Rosas](#) ,  
[Santiago González-Periañez](#) , [Ezri Cruz-Pérez](#) , [Tushar Janardan Pawar](#) <sup>\*</sup> , [Fernando Rafael Ramos-Morales](#) <sup>\*</sup>

Posted Date: 26 June 2025

doi: [10.20944/preprints202506.2064.v1](https://doi.org/10.20944/preprints202506.2064.v1)

Keywords: *Justicia spicigera*; prostate cancer; LNCaP cells; kaempferitrin; ethnopharmacology; plant-derived anticancer agents



Preprints.org is a free multidisciplinary platform providing preprint service that is dedicated to making early versions of research outputs permanently available and citable. Preprints posted at Preprints.org appear in Web of Science, Crossref, Google Scholar, Scilit, Europe PMC.

Copyright: This open access article is published under a Creative Commons CC BY 4.0 license, which permit the free download, distribution, and reuse, provided that the author and preprint are cited in any reuse.

Disclaimer/Publisher's Note: The statements, opinions, and data contained in all publications are solely those of the individual author(s) and contributor(s) and not of MDPI and/or the editor(s). MDPI and/or the editor(s) disclaim responsibility for any injury to people or property resulting from any ideas, methods, instructions, or products referred to in the content.

## Article

# Cytostatic Effects of Hydroalcoholic Extract of *Justicia spicigera* on LNCaP Prostate Cancer Cells: Cell Cycle Arrest and Apoptosis Induction

Ivette Bravo-Espinoza <sup>1,2,†</sup>, Fabiola Hernández-Rosas <sup>3,4,5,†</sup>, María Elena Hernández-Aguilar <sup>2</sup>, Marycarmen Godínez-Victoria <sup>6</sup>, Rodrigo Rafael Ramos-Hernández <sup>7</sup>, Carlos Alberto López-Rosas <sup>1,7,8</sup>, Santiago González-Periañez <sup>7,9</sup>, Ezri Cruz-Pérez <sup>1</sup>, Tushar Janardan Pawar, <sup>10,11,\*</sup> and Fernando Rafael Ramos-Morales <sup>1,7,\*</sup>

<sup>1</sup> Facultad de Química Farmacéutica Biológica, Universidad Veracruzana, Circuito Gonzalo Aguirre Beltrán s/n, Zona Universitaria, 91090 Xalapa-Enríquez, Veracruz, México

<sup>2</sup> Instituto de Investigaciones Cerebrales, Universidad Veracruzana, Luis Castelazo Ayala s/n, Col. Industrial Animas, 91190 Xalapa-Enríquez, Veracruz, México

<sup>3</sup> Centro de Investigación, Universidad Anáhuac Querétaro, El Marqués, Querétaro 76246, Mexico

<sup>4</sup> Escuela de Ingeniería Biomédica, División de Ingenierías, Universidad Anáhuac Querétaro, El Marqués, Querétaro 76246, Mexico

<sup>5</sup> Facultad de Química, Universidad Autónoma de Querétaro, Querétaro 76010, Mexico

<sup>6</sup> Sección de Estudios de Posgrado e Investigación, Escuela Superior de Medicina, Instituto Politécnico Nacional, Mexico City, Mexico

<sup>7</sup> Instituto de Química Aplicada, Universidad Veracruzana, Luis Castelazo Ayala s/n, Col. Industrial Animas, 91190 Xalapa-Enríquez, Veracruz, México

<sup>8</sup> Instituto de Neuroetología, Universidad Veracruzana, Luis Castelazo Ayala s/n, Col. Industrial Animas, Xalapa 91190, México

<sup>9</sup> Facultad de Bioanálisis, Universidad Veracruzana, Calle Médicos y Odontólogos s/n, Unidad del Bosque, C.P. 91010. Xalapa-Enríquez, Veracruz, México

<sup>10</sup> Red de Estudios Moleculares Avanzados, Campus III, Instituto de Ecología A. C., Carretera Antigua a Coatepec 351, Xalapa, 91073, Veracruz, México

<sup>11</sup> Unidad de Desarrollo e Investigación en Bioterapéuticos (UDIBI), Escuela Nacional de Ciencias Biológicas, Instituto Politécnico Nacional, 11340 Mexico City, Mexico

\* Correspondence: tushar.janardan@inecol.mx (T.J.P.); framos@uv.mx (F.R.R.-M.)

† Authors have equal contributions.

## Abstract

*Justicia spicigera*, a medicinal plant traditionally used in Mexican ethnomedicine, remains underexplored for its potential anticancer activity against prostate cancer. This study evaluates the cytostatic and apoptotic effects of a hydroalcoholic extract of *J. spicigera* on androgen-sensitive LNCaP prostate cancer cells. Phytochemical characterization via TLC, HPLC, LC-MS, and NMR confirmed the presence of kaempferitrin,  $\beta$ -sitosterol, and cryptoxanthin derivatives. Dose-dependent antiproliferative effects were observed in MTT and trypan blue assays, with significant cytotoxicity emerging at  $\geq 500$   $\mu$ g/mL. Flow cytometry revealed G<sub>0</sub>/G<sub>1</sub> cell cycle arrest at 250  $\mu$ g/mL and marked apoptosis at 500  $\mu$ g/mL and above, as evidenced by Annexin V/PI staining. At lower doses, the extract exhibited a cytostatic effect, inhibiting proliferation without inducing apoptosis. The dual behavior suggests that the extract modulates cell cycle checkpoints and apoptotic pathways in a dose-dependent manner. Unlike conventional chemotherapeutics, *J. spicigera* may offer a less toxic alternative by selectively impairing tumor cell proliferation at sub-lethal concentrations. The observed dose-dependent effects open new avenues for investigating plant-derived compounds as modulators of prostate cancer cell proliferation and survival.

**Keywords:** *Justicia spicigera*; prostate cancer; LNCaP cells; kaempferitrin; ethnopharmacology; plant-derived anticancer agents

---

## 1. Introduction

Prostate cancer is one of the most commonly diagnosed malignancies in men and remains a significant contributor to cancer-related mortality worldwide. Benign prostatic hyperplasia and prostate cancer are among the most common diseases of the prostate gland and represent significant burdens for patients and health-care systems in many countries, as Mexico. In 2023, 133,539 cases of prostate hyperplasia were reported, and in 2024, there were 123,215. The rates are 638.8 per 100,000 inhabitants and 589.4 per 100,000 men over 40 years of age. Regarding prostate cancer, 5,062 cases were reported in 2023. In 2024, there were 6,050. The rates are 24.2 per 100,000 inhabitants and 28.9 per 100,000 men over 40 years of age [1]. Prostate cancer deaths in Mexico in 2023 were 7,241. The mortality rate was 34.6 per 100,000 men over 40 years of age [2]. It is a highly heterogeneous disease, progressing through localized, advanced, and metastatic stages, each requiring distinct therapeutic strategies [3]. While genetic predisposition and environmental factors play a role in disease onset, mutations in genes such as BRCA1, BRCA2, and TP53, which regulate androgen metabolism and DNA repair, significantly contribute to prostate cancer development and progression [4]. The androgen receptor (AR) signaling pathway is central to prostate cancer biology, making it a key therapeutic target. Conventional treatment strategies, including androgen deprivation therapy (ADT), chemotherapy, and immunotherapy, have demonstrated efficacy; however, drug resistance and treatment-associated toxicities pose significant challenges, emphasizing the need for alternative or complementary therapeutic approaches [5].

Traditional medicine has historically played an essential role in cancer treatment, with medicinal plants serving as a primary source of bioactive compounds for drug discovery. Many FDA-approved anticancer agents, including paclitaxel, vinblastine, and camptothecin, are derived from natural products, highlighting their importance in modern oncology [6]. These limitations underscore the need for alternative strategies, including the use of medicinal plants that offer low toxicity and broader accessibility. *Justicia spicigera*, a plant widely used in Mexican ethnomedicine, has attracted scientific interest due to its diverse bioactive compounds, including flavonoids, phytosterols, and anthocyanins, which exhibit anticancer, anti-inflammatory, and immunomodulatory properties [7–9]. While previous studies have reported that kaempferitrin, a key flavonoid in *J. spicigera*, induces apoptosis in various cancer models, its precise effects on prostate cancer cells remain largely unexplored. Given that prostate cancer treatment resistance is often linked to evasion of apoptosis, investigating whether *J. spicigera* influences cell cycle progression or apoptotic pathways in LNCaP cells is essential. Many plant-derived compounds influence cancer progression by modulating the cell cycle, inducing apoptosis, or targeting signaling pathways central to tumor survival and proliferation. [10].

The Acanthaceae family, to which *Justicia spicigera* Schleidl. belongs, includes more than 600 species used in traditional medicine for various ailments, including inflammation, infections, and metabolic disorders [11,12]. In Mexican ethnomedicine, *J. spicigera* has been widely utilized for treating anemia, menstrual irregularities, respiratory diseases, and microbial infections [13–15]. However, despite its broad therapeutic applications, research on its potential anticancer effects remains limited.

Several studies have reported the presence of flavonoids, phytosterols, and terpenoids in *J. spicigera*, many of which exhibit promising anticancer properties [16–19]. Kaempferitrin and quercetin derivatives, found in *J. spicigera*, have demonstrated antiproliferative and apoptotic activity, acting through the modulation of p53, Bcl-2, Bax, and cyclins, which regulate cell cycle progression and programmed cell death [20]. Additionally,  $\beta$ -sitosterol, a major phytosterol in *J. spicigera*, has been shown to inhibit prostate cancer cell proliferation by modulating ceramide metabolism and AR signaling [21].



Although the cytotoxic effects of *J. spicigera* have been reported in leukemia (TF-1), cervical (HeLa), and breast (T47D) cancer cells [22,23], its potential cytotoxic effect in prostate cancer, particularly in androgen-sensitive models like LNCaP, remains largely unexplored. Previous studies have demonstrated that *J. spicigera* extract induces apoptosis at low micromolar concentrations, with  $IC_{50}$  values as low as 17  $\mu$ g/mL in HeLa cells [24]. Additionally, an *in vivo* study showed that *J. spicigera* extract suppressed tumor growth by up to 53%, comparable to the effects of cisplatin, suggesting significant anticancer potential [25].

One of the major challenges in prostate cancer therapy is overcoming drug resistance and systemic toxicity associated with conventional treatments [5]. Many standard chemotherapeutics exert their effects by inducing direct cytotoxicity, leading to significant side effects and the selection of resistant cancer cell populations. In contrast, cytostatic agents, which inhibit cell proliferation without immediately triggering apoptosis, offer an alternative approach that may delay tumor progression and reduce therapy resistance.

Given the growing interest in plant-derived cytostatic compounds, it is critical to investigate whether *J. spicigera* primarily acts via cell cycle modulation or through direct apoptosis induction. The presence of flavonoids and sterols in *J. spicigera* suggests a possible mechanism involving  $G_0/G_1$  arrest and subsequent apoptosis induction, as previously demonstrated in other plant-derived anticancer compounds [25]. However, no study has comprehensively evaluated these effects in prostate cancer models, warranting further investigation.

Despite preliminary evidence of anticancer activity, studies assessing *J. spicigera* in prostate cancer models, especially in androgen-responsive LNCaP cells remain scarce. A prior study by [26] reported that *J. spicigera* extract induced a modest  $G_0$ -phase cell cycle arrest in LNCaP cells at high concentrations ( $IC_{50} = 3026 \pm 421 \mu$ g/mL) but lacked significant apoptotic effects. The limited apoptotic response observed in earlier studies prompts a closer examination of whether *J. spicigera* can activate programmed cell death pathways at lower, therapeutically relevant concentrations, an aspect that has not been thoroughly addressed to date.

This study aims to evaluate the effects of hydroalcoholic extract of *J. spicigera* on LNCaP prostate cancer cells, with a specific focus on phytochemical composition analysis (flavonoids, phytosterols, terpenoids), cytostatic vs. cytotoxic mechanisms (MTT, trypan blue exclusion assays) and cell cycle progression and apoptosis (flow cytometry, Annexin V/PI staining). By elucidating the effects of *J. spicigera* on cell proliferation, cell cycle regulation, and apoptotic pathways, this study contributes to the evidence-based validation of traditional medicinal plants in cancer therapy. Furthermore, understanding whether *J. spicigera* acts as a cytostatic agent rather than a direct cytotoxin may have important implications for developing alternative prostate cancer treatments with reduced side effects.

## 2. Results and Discussion

### 2.1. Phytochemical Characterization of *Justicia spicigera* Extract

The hydroalcoholic extract of *Justicia spicigera* was analyzed using a combination of chromatographic and spectroscopic techniques to identify its major bioactive constituents. The extract revealed a complex phytochemical profile rich in flavonoids, phytosterols, and carotenoid derivatives, which have been historically associated with the plant's traditional medicinal use in Mexican ethnobotany [7].

The complete results of TLC, HPLC, MS and NMR are reported in the Supporting Material. Thin-layer chromatography (TLC) analysis confirmed the presence of flavonoids and saponins, with distinct fluorescent bands observed under UV 365 nm following post-spraying with aluminum chloride and sulfuric acid. These fluorescence signatures are consistent with flavonoid glycosides previously reported in *J. spicigera*, including kaempferitrin and quercetin derivatives [17,25].

High-performance liquid chromatography with diode-array detection (HPLC-DAD) showed a prominent peak at a retention time of ~12.8 min with a UV absorption maximum at 348 nm, consistent

with kaempferol-based flavonoids. Further identification was performed using LC-MS in positive ion mode, where extracted ion chromatograms (EICs) revealed molecular ions at  $m/z$  579.1 ( $[M+H]^+$ ) corresponding to kaempferitin, along with signals at  $m/z$  433.1 and 453.3, consistent with additional flavonoid and sterol-related metabolites.

Mass spectral fragmentation patterns supported the identification of other compounds, including  $\beta$ -sitosterol ( $m/z$  414.7), allantoin ( $m/z$  157.1), and cryptoxanthin derivatives ( $m/z$  552.9), all of which are known for antioxidant and anticancer potential [20].

Structural confirmation of kaempferitin was achieved via  $^1$ H-NMR spectroscopy. The spectrum displayed characteristic aromatic proton signals in the  $\delta$  6.2–7.8 ppm range, alongside glucose anomeric protons at  $\delta$  5.1–5.6 ppm. For  $\beta$ -sitosterol, methyl group signals appeared at  $\delta$  0.8–1.2 ppm, and the hydroxyl proton was detected at  $\delta$  3.5 ppm, consistent with published data [27].

Collectively, the analytical results point to kaempferitin as the principal flavonoid component in the extract, accompanied by  $\beta$ -sitosterol and carotenoid derivatives. These metabolites have been previously implicated in redox balance, apoptotic signaling, and cell cycle regulation, providing a rational biochemical basis for the cellular responses observed in the LNCaP model, as explored in subsequent sections [25].

## 2.2. Effects of *J. spicigera* on LNCaP Cell Proliferation

To investigate the antiproliferative effects of *J. spicigera* extract, a combination of colorimetric and microscopic assays was used to assess cell viability, morphology, and membrane integrity. The results collectively demonstrate a dose- and time-dependent inhibition of LNCaP cell proliferation, with evidence of cytostatic effects at sub-lethal concentrations and cytotoxic responses at higher doses.

### 2.2.1. MTT Assay

The metabolic activity of LNCaP cells was evaluated using the MTT assay after exposure to be increasing concentrations of *J. spicigera* extract (62.5–4000  $\mu$ g/mL) for 24, 48, and 72 h. At 250  $\mu$ g/mL, no significant reduction in viability was observed at 24 h, suggesting minimal cytotoxicity at this concentration. However, at 500  $\mu$ g/mL, a marked reduction in cell viability was detected ( $p < 0.001$ ), which became more pronounced at extended time points. At higher concentrations (1000–4000  $\mu$ g/mL), viability decreased to below 20% by 72 h, closely resembling the effect of the positive control etoposide (10  $\mu$ M) (Figure 1).

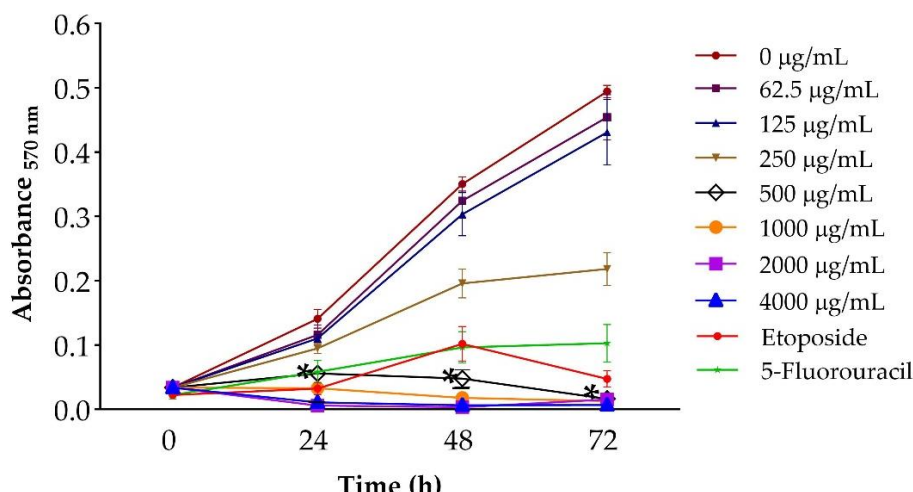


**Figure 1.** MTT assay results for LNCaP cells treated with *J. spicigera* extract at increasing concentrations (62.5–4000  $\mu$ g/mL) for 24, 48, and 72 hours. Values are expressed as mean  $\pm$  SEM ( $n = 9$ ). \*( $p < 0.001$ ).

### 2.2.2. Morphological Characterization of Treated LNCaP Cells

To complement the metabolic viability data, phase-contrast microscopy was performed to assess the morphological changes induced by the extract. Untreated control cells maintained a polygonal epithelial morphology with dense, adherent colonies typical of LNCaP cells.

Following treatment with 250  $\mu$ g/mL extract, cells exhibited slight reductions in colony density and spreading at 48 h, without evidence of membrane disruption or blebbing—findings consistent with a cytostatic response. In contrast, cells exposed to 500  $\mu$ g/mL showed early signs of apoptosis as early as 24 h, including cell shrinkage, rounding, and partial detachment from the substrate. These changes intensified at 48 h, marked by pronounced membrane blebbing and disruption of the monolayer (Figure 2).

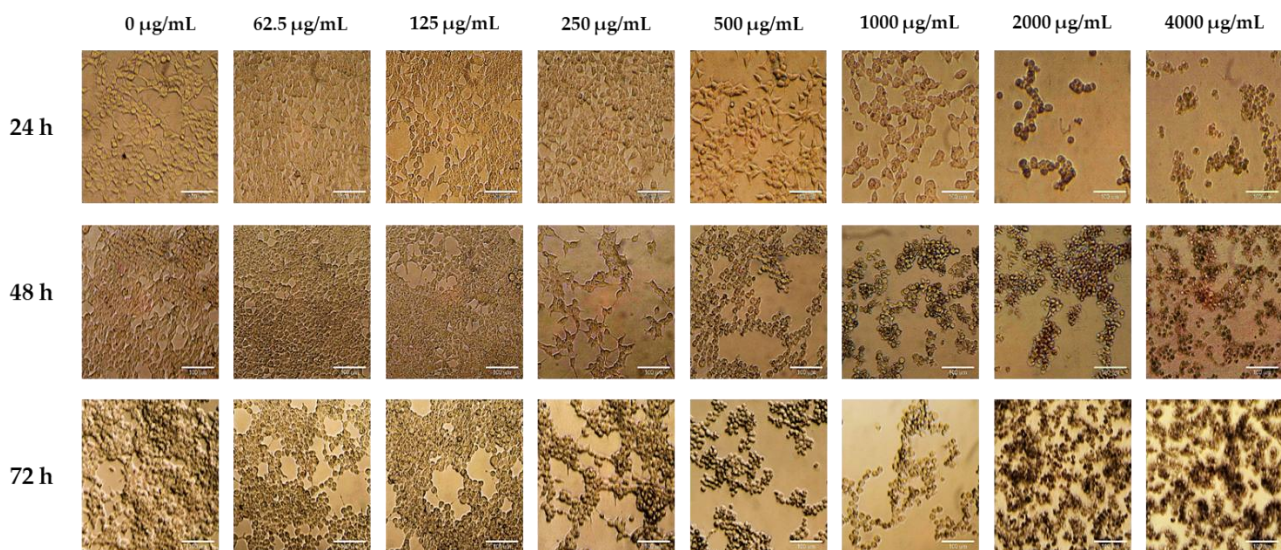


**Figure 2.** Morphological analysis of LNCaP cells treated with *Justicia spicigera* extract at 250 and 500  $\mu$ g/mL for 24 h, 48 h and 72 h. Representative phase-contrast micrographs demonstrate dose- and time-dependent morphological changes, including cell rounding, detachment, and reduced adherence. Scale bar = 100  $\mu$ m.

### 2.2.3. Trypan Blue Assay

To directly assess membrane integrity and distinguish viable from non-viable cells, the trypan blue exclusion assay was conducted under the same treatment conditions. At 250  $\mu$ g/mL, no significant reduction in viable cell counts was observed at 24 h, while a modest but significant decline emerged by 48 h ( $p < 0.05$ ), consistent with delayed cytostatic effects. At 500  $\mu$ g/mL, viability dropped sharply at 48 and 72 h ( $p < 0.001$ ), corroborating the cytotoxic threshold observed in MTT (Figure 3A) and morphological analyses (Figure 3B).

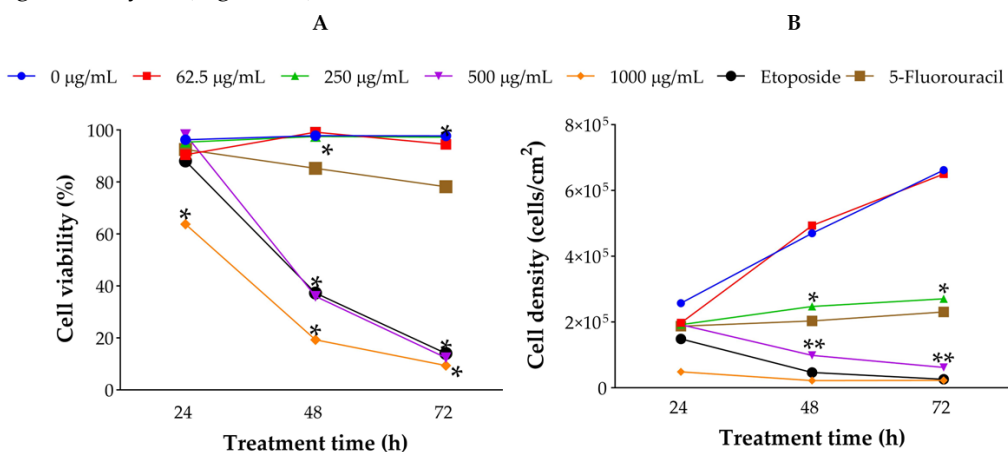


**Figure 3.** Trypan blue exclusion assay results showing viable and non-viable LNCaP cells after treatment with *J. spicigera* extract at 24, 48, and 72 hours. Values represent mean  $\pm$  SEM ( $n = 9$ ). Statistical significance: (\* $p < 0.05$ , \*\* $p < 0.001$ ).

The data collectively reveals a concentration-dependent shift in cellular response. At doses up to 250  $\mu$ g/mL, *J. spicigera* extract limits proliferation without compromising membrane integrity, consistent with a cytostatic effect likely driven by reduced metabolic activity or signaling interference. At concentrations of 500  $\mu$ g/mL and above, pronounced morphological changes, loss of membrane integrity, and reduced viability indicate a cytotoxic response, likely mediated by apoptosis. This dual behavior suggests that distinct molecular pathways may be engaged depending on the dose, warranting closer examination of apoptotic signaling and cell cycle regulation in subsequent analyses.

### 2.3. Apoptosis Induction and Cell Viability

*J. spicigera* extract induced apoptosis in LNCaP cells in a dose-dependent manner, as determined by Annexin V/PI staining and flow cytometry analysis (Figure 4). At 250  $\mu$ g/mL, the percentage of apoptotic cells remained comparable to that of untreated controls, confirming that this concentration primarily exerts a cytostatic rather than cytotoxic effect. However, at 500  $\mu$ g/mL, a significant increase in early apoptosis was observed at 24 h, progressing to late apoptosis at 48 h ( $p < 0.001$  vs. control). At concentrations of 1000  $\mu$ g/mL and above, apoptosis was predominant, with a concurrent increase in necrotic cell death, similar to the effect observed with etoposide (positive control).

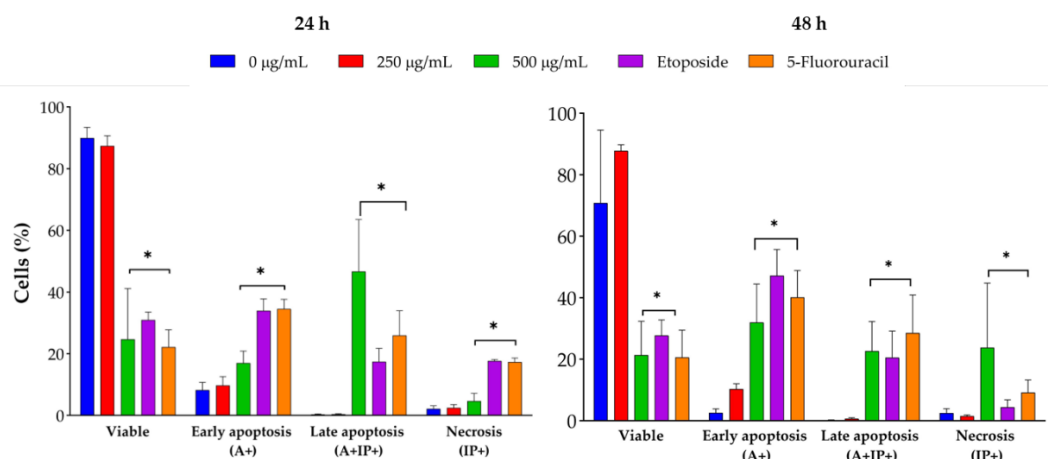


**Figure 4.** Flow cytometry analysis of LNCaP cells treated with *J. spicigera* extract at 250, 500, and 1000  $\mu$ g/mL for 24 and 48 hours. Apoptotic cells were detected using Annexin V/PI staining. Bars represent mean  $\pm$  SEM ( $n = 3$ ). (\* $p < 0.001$ ).

The dot plots showing Annexin V/PI staining at 24 and 48 h provide visual confirmation of the dose-dependent shift from viability to apoptosis. At 24 h, a shift from viable to apoptotic quadrants was evident at  $\geq 500$   $\mu$ g/mL. At 48 h, the shift was more pronounced, with the highest concentrations inducing widespread late apoptosis and necrosis, while 250  $\mu$ g/mL maintained a largely viable profile (Figure 5 and 6).

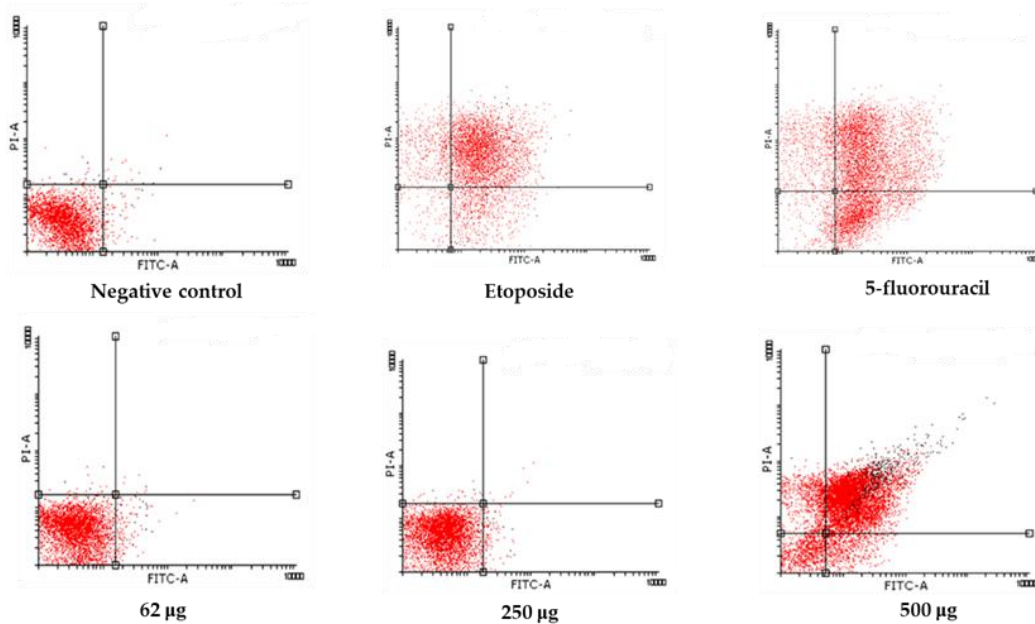


**Figure 5.** Annexin V-FITC/PI dot plots of LNCaP cells at 24 h. Treatments include control, 62.5  $\mu$ g/mL, 250  $\mu$ g/mL, 500  $\mu$ g/mL, and positive controls (etoposide and 5-fluorouracil). Apoptotic populations shift toward the lower-right and upper-right quadrants in a dose-dependent manner.

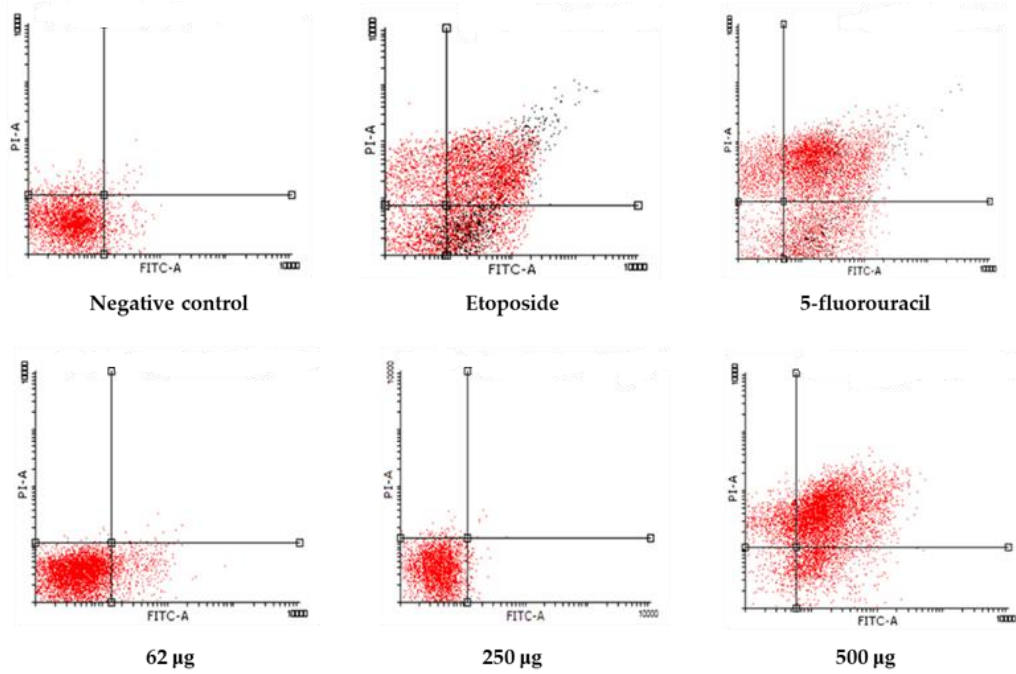


**Figure 6.** Annexin V-FITC/PI dot plots of LNCaP cells at 48 h. Apoptotic and necrotic populations increase with extract concentration and are most pronounced at 500  $\mu$ g/mL and 1000  $\mu$ g/mL. Positive controls show widespread cell death, while 250  $\mu$ g/mL retains a predominantly viable profile.

Interestingly, at 250  $\mu$ g/mL, apoptosis was not significantly induced, further supporting the hypothesis that this concentration primarily induces cell cycle arrest rather than direct cytotoxicity, a desirable characteristic for therapies aimed at controlling tumor progression with minimal toxicity.

To determine whether the observed reduction in cell proliferation was due to apoptosis rather than loss of membrane integrity, flow cytometry with propidium iodide (PI) exclusion was conducted (Figure 7). PI exclusion distinguishes viable cells (PI-negative) from necrotic and late apoptotic cells (PI-positive).

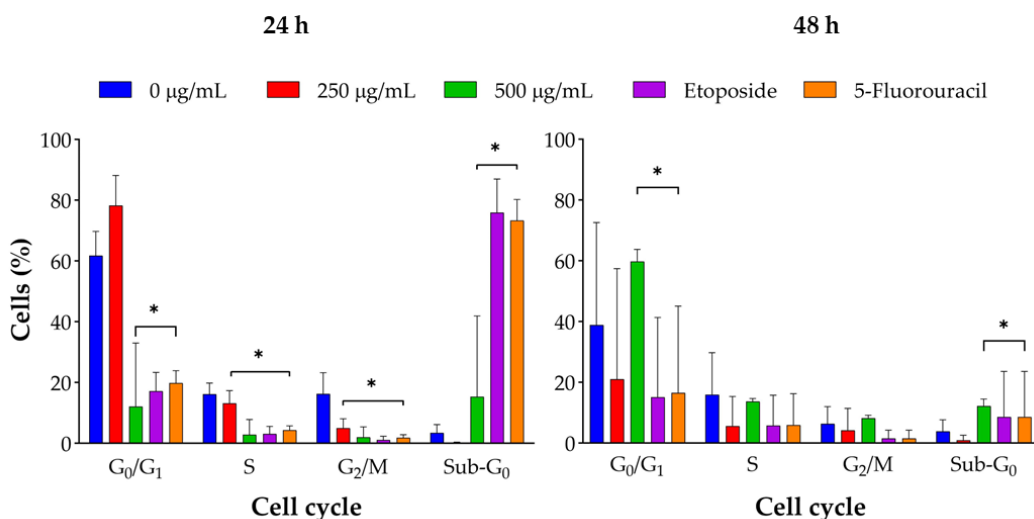


**Figure 7.** Cell viability assessment of LNCaP cells treated with *J. spicigera* extract at various concentrations using flow cytometry and PI exclusion assay. Data are presented as mean  $\pm$  SEM ( $n = 3$ ). (\* $p < 0.001$ ).

At 250  $\mu$ g/mL, the percentage of viable cells remained above 85% at 24 and 48 h, reinforcing the evidence that this concentration primarily exerts a cytostatic rather than cytotoxic effect. However, at 500  $\mu$ g/mL, a significant reduction in viable cell populations was observed by 48 h, with a notable increase in apoptotic cells ( $p < 0.001$ ). At 1000  $\mu$ g/mL, cell viability dropped dramatically, with a substantial transition to late apoptosis or necrosis.

Collectively, the flow cytometry and viability data indicate that apoptosis is the predominant mode of cell death at concentrations  $\geq$ 500  $\mu$ g/mL, while 250  $\mu$ g/mL primarily maintains membrane integrity and cell viability. This concentration-dependent transition from cytostasis to apoptosis aligns with the presence of flavonoids and phytosterols in the extract, compounds previously reported to modulate apoptotic signaling and mitochondrial function in cancer cells [23,24].

The pattern of Annexin V positivity, sub-G<sub>0</sub>/G<sub>1</sub> accumulation, and loss of membrane integrity suggests activation of caspase-dependent apoptosis. Although not directly measured in this study, the presence of kaempferitrin, cryptoxanthin, and  $\beta$ -sitosterol may account for the observed effects, given their documented roles in oxidative stress modulation and pro-apoptotic signaling [28–39]. Further validation through molecular assays targeting Bcl-2, Bax, and caspase pathways is warranted to delineate the apoptotic mechanisms in LNCaP cells.

#### 2.4. Cell Cycle Arrest Mechanism

Flow cytometry analysis indicated that *J. spicigera* extract induced dose-dependent changes in the cell cycle distribution of LNCaP cells. At 250  $\mu$ g/mL, a significant accumulation of cells in the G<sub>0</sub>/G<sub>1</sub> phase was observed, alongside a reduction in the S phase population ( $p < 0.01$ ). This pattern intensified at 500  $\mu$ g/mL, with increased G<sub>0</sub>/G<sub>1</sub> arrest, further S phase depletion, and a notable rise in the sub-G<sub>0</sub>/G<sub>1</sub> fraction, consistent with DNA fragmentation and the onset of apoptosis ( $p < 0.001$ ). At 1000  $\mu$ g/mL, the sub-G<sub>0</sub>/G<sub>1</sub> population became dominant, indicating that apoptotic cell death supersedes cytostatic effects at higher concentrations.

The shift from G<sub>0</sub>/G<sub>1</sub> arrest to apoptosis with increasing extract concentrations suggests a sequential mechanism, where sustained cell cycle inhibition leads to loss of viability. This transition reflects a characteristic mode of action observed in several plant-derived flavonoids that target cell cycle regulators and DNA integrity pathways [22]. Compared to conventional chemotherapeutics, which often cause G<sub>2</sub>/M arrest, the preferential G<sub>0</sub>/G<sub>1</sub> arrest observed with *J. spicigera* may offer a different point of intervention, particularly relevant to hormone-sensitive and AR-independent forms of prostate cancer [40].

The observed cell cycle arrest, supported by concurrent viability and apoptosis assays, points to interference with cyclin D1/CDK4 and other early G<sub>1</sub>-phase regulators [25]. While not directly assessed here, these results provide a rationale for future experiments aimed at profiling the expression and activity of CDKs, Rb, and p21 in response to extract treatment. Comparative analysis with normal prostate epithelial cells will be essential to confirm whether this mechanism confers selectivity toward malignant cells.

## 2.5. Mechanistic Basis & Therapeutic Relevance

Based on the combined evidence from cell viability, apoptosis, and cell cycle assays, *Justicia spicigera* extract modulates LNCaP prostate cancer cell behavior in a concentration-dependent manner (Figure 8). At 250 µg/mL, the extract consistently induced G<sub>0</sub>/G<sub>1</sub> arrest without triggering apoptosis, indicating interference with early cell cycle checkpoints rather than direct cytotoxicity. In contrast, concentrations ≥500 µg/mL produced clear apoptotic responses, including phosphatidylserine translocation, sub-G<sub>0</sub>/G<sub>1</sub> accumulation, and DNA fragmentation. This transition aligns with mitochondrial dysfunction and caspase activation observed in other cancer models treated with flavonoid-rich extracts.

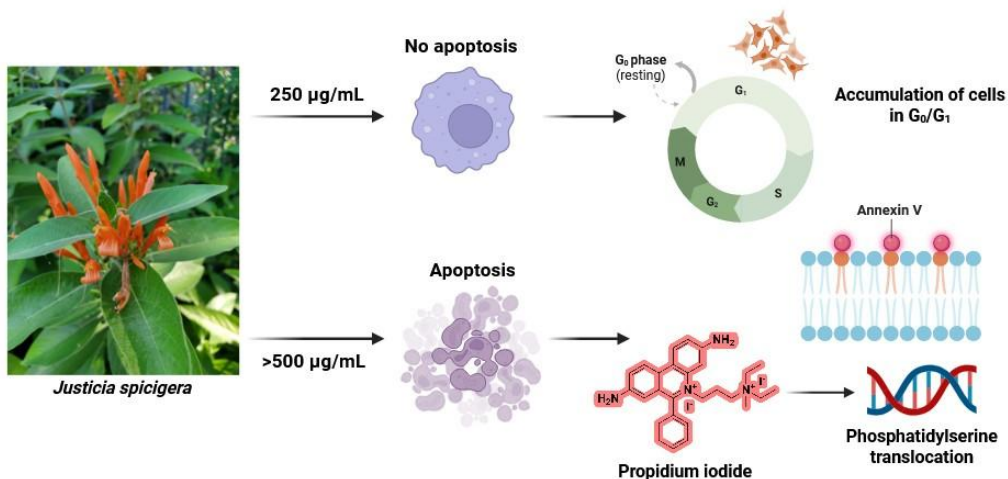


**Figure 8.** Proposed model of the dose-dependent effect of *Justicia spicigera* extract on LNCaP prostate cancer cells. At 250 µg/mL, the extract induces G<sub>0</sub>/G<sub>1</sub> arrest, reducing proliferation without triggering apoptosis. At higher concentrations (≥500 µg/mL), it initiates apoptosis through phosphatidylserine translocation, caspase activation, and DNA fragmentation.

Phytochemical profiling identified kaempferitrin, β-sitosterol, and cryptoxanthin derivatives as principal constituents. These compounds have been implicated in modulating PI3K/Akt, p53, and MAPK pathways, all of which influence apoptotic regulation and cell cycle progression. Kaempferitrin and quercetin analogs have been shown to alter cyclin D1/CDK4 activity and trigger mitochondrial depolarization. Likewise, β-sitosterol may contribute through AR axis interference and modulation of lipid-mediated signaling.

The selective induction of cell cycle arrest at lower doses, coupled with apoptosis at higher concentrations, suggests a tiered mechanism of action not commonly observed in conventional chemotherapeutics. Such agents typically exert immediate cytotoxic effects and often compromise normal proliferative tissues. The apparent retention of cell viability at 250 µg/mL, alongside suppressed proliferation, may represent a more controlled growth-inhibitory profile, potentially minimizing collateral damage to non-malignant cells.

Collectively, the observed responses in LNCaP cells, anchored in defined biochemical and morphological changes support a mechanistic framework in which *J. spicigera* targets both proliferative signaling and apoptotic regulation. These results offer a biochemical rationale for further

validation using molecular assays of key targets such as p21, p53, and cyclin D1, and raise the possibility of future testing in prostate cancer models resistant to current hormone-based therapies.

## 4. Materials and Methods

### 4.1. Plant Material and Extract Preparation

Fresh aerial parts of *J. spicigera* were collected from Lencero, Veracruz, México ( $19^{\circ} 29' 27.5''$  N,  $96^{\circ} 48' 53.6''$  W) in February 2021. The plant was taxonomically identified by Dr. Edison Fernando Nicolalde Morejón, a plant taxonomist at Universidad Veracruzana, and a voucher specimen (No. 15655) was deposited at the Herbarium of Instituto de Investigaciones Biológicas, Universidad Veracruzana, for future reference.

The collected plant material was washed with distilled water, air-dried at room temperature ( $25^{\circ}\text{C}$ , 50–60% relative humidity) for seven days, and manually cut into small pieces. Hydroalcoholic extraction was performed by macerating 90 g of powdered plant material in 500 mL ethanol:water (50:50) at room temperature for 72 h with occasional stirring. The extract was filtered using Whatman No. 1 filter paper, concentrated under reduced pressure using a rotary evaporator (Büchi R-210) at  $40^{\circ}\text{C}$ , and lyophilized in a freeze dryer (Labconco FreeZone 4.5 and 117) to obtain a dry extract. These results strongly suggest that kaempferitrin is the predominant bioactive flavonoid in *J. spicigera*, with additional contributions from sterols and carotenoids. The documented ability of kaempferitrin to induce apoptosis and arrest the cell cycle in cancer models [41] suggests that its presence may contribute to the extract's potential anticancer effects. Given that flavonoids and phytosterols have been widely studied for their anticancer mechanisms, these results provide further evidence that traditional medicinal uses of *J. spicigera* may be supported by its biochemical composition [7].

For cell-based assays, the extract was reconstituted in RPMI-1640 culture medium to achieve the desired working concentrations.

### 4.2. Phytochemical Characterization

The phytochemical composition of *J. spicigera* hydroalcoholic extract was analyzed using TLC, HPLC, LC-MS, and NMR spectroscopy. These analytical techniques enabled the identification and structural elucidation of bioactive compounds.

TLC was performed using silica gel 60 F254 plates (Merck) as the stationary phase. The extract (5  $\mu\text{L}$ ) was applied as a spot and developed in a 1-butanol:water:acetic acid (6:3:1) solvent system. Plates were visualized under UV light (254 nm and 365 nm), followed by spraying with natural product reagent (NP/PEG; diphenylboric acid- $\beta$ -ethylamino ester/polyethylene glycol, Sigma-Aldrich) to detect flavonoids. The R<sub>f</sub> values of detected bands were recorded.

HPLC analysis was conducted using an Agilent 1260 Infinity HPLC system (Agilent Technologies) equipped with a photodiode array (PDA) detector. Separation was performed on a C18 column (250 mm  $\times$  4.6 mm, 5  $\mu\text{m}$ , Phenomenex) at  $30^{\circ}\text{C}$ . The mobile phase consisted of 0.1% formic acid in water (solvent A) and acetonitrile (solvent B) with a gradient elution program. The injection volume was 10  $\mu\text{L}$ , and detection wavelengths were set at 254 nm and 365 nm for flavonoids, and 210 nm for sterols. Retention times were compared with reference standards for compound identification.

LC-MS analysis was performed using an Agilent 6545 Q-TOF LC-MS system (Agilent Technologies) with an electrospray ionization (ESI) source. The instrument was operated in positive and negative ionization modes, scanning an m/z range of 100–1000 Da. The capillary voltage was set at 3.5 kV, with a nebulizer gas pressure of 45 psi and a desolvation temperature of  $350^{\circ}\text{C}$ . Fragmentation patterns were analyzed using collision-induced dissociation (CID) at 20 eV, and spectral data were processed using MassHunter software (Agilent Technologies).

For structural elucidation, <sup>1</sup>H-NMR and <sup>13</sup>C-NMR spectroscopy were conducted. The extract was dissolved in deuterated dimethyl sulfoxide (DMSO-d<sub>6</sub>, Sigma-Aldrich) at 10 mg/mL and analyzed using a Bruker Avance III 600 MHz NMR spectrometer. <sup>1</sup>H-NMR spectra were recorded with a 12 ppm sweep width, while <sup>13</sup>C-NMR spectra were acquired using broadband proton decoupling.

Chemical shifts ( $\delta$  values) were reported in ppm, and coupling constants ( $J$  values) were measured in Hz.

#### 4.3. Cell Culture and Maintenance

The human prostate cancer cell line LNCaP (ATCC® CRL-1740™) was obtained from ATCC and maintained in RPMI-1640 medium (Gibco) supplemented with 10% fetal bovine serum (FBS, Gibco), 1% penicillin-streptomycin (Sigma-Aldrich), and 2 mM L-glutamine (Gibco). Cells were incubated at 37°C in a humidified atmosphere with 5% CO<sub>2</sub> and passaged every 2–3 days upon reaching 70–80% confluence using 0.25% trypsin-EDTA (Gibco).

Cell viability was monitored using the trypan blue exclusion assay, and only cultures with ≥95% viability were used for experiments. The absence of Mycoplasma contamination was routinely verified using a PCR-based Mycoplasma detection kit (Lonza).

For experimental treatments, LNCaP cells were seeded into 96-well, 12-well, or 6-well plates, depending on the assay requirements, and allowed to adhere for 24 h before treatment. Cells were then treated with varying concentrations of *J. spicigera* extract, while 0.1% DMSO served as the vehicle control (negative control).

#### 4.4. MTT Assay for Cell Viability

The MTT assay was used to evaluate the effect of *J. spicigera* extract on LNCaP cell viability. This colorimetric assay measures the reduction of MTT into formazan crystals by mitochondrial dehydrogenases in metabolically active cells, with absorbance intensity correlating with the number of viable cells.

LNCaP cells were seeded in 96-well plates at  $8 \times 10^4$  cells per well in 100  $\mu$ L of RPMI-1640 medium and allowed to adhere for 24 h at 37°C in a 5% CO<sub>2</sub> incubator. After adherence, cells were treated with serial dilutions of *J. spicigera* extract for 24, 48, and 72 h, with 0.1% DMSO serving as the vehicle control. Each condition was tested in triplicate wells across three independent experiments.

Following the incubation period, 10  $\mu$ L of MTT (M2128, Sigma-Aldrich) solution (5 mg/mL in PBS, Sigma-Aldrich) was added to each well, and plates were incubated for 3 h at 37°C. The supernatant was removed, and 100  $\mu$ L of DMSO (Sigma-Aldrich) was added to dissolve the formazan crystals. Absorbance was measured at 570 nm, with background correction at 650 nm, using a microplate reader (Multiskan GO, Thermo Fisher Scientific).

Cell viability was calculated relative to the untreated control using the formula:

$$\text{Cell viability (\%)} = \frac{\text{Absorbance of treated cells}}{\text{Absorbance of control cells}} \times 100$$

#### 4.5. Trypan Blue Exclusion Assay

The Trypan Blue exclusion assay was used to assess LNCaP cell viability following treatment with *J. spicigera* extract. This method differentiates between viable and non-viable cells, as intact plasma membranes exclude Trypan Blue, whereas compromised membranes allow dye uptake, making non-viable cells appear blue under a microscope.

LNCaP cells were seeded in 12-well plates at  $1 \times 10^5$  cells per well in 1 mL of RPMI-1640 medium (R8005, Sigma-Aldrich) and allowed to adhere for 24 h at 37°C in a humidified incubator with 5% CO<sub>2</sub>. After adherence, cells were treated with varying concentrations of *J. spicigera* extract, with 0.1% DMSO as the vehicle control, 10  $\mu$ M etoposide (Sigma-Aldrich) and 5-fluorouracil as the positive controls. Each condition was tested in triplicate wells across three independent experiments.

At the end of the incubation period, the culture medium was removed, and cells were trypsinized with 0.25% Trypsin-EDTA (Gibco) for 2 min at 37°C. Trypsinization (T3924, Sigma-Aldrich) was halted by adding an equal volume of complete RPMI-1640 medium (10% FBS), and cells were resuspended in PBS. A 10  $\mu$ L aliquot of the suspension was mixed with 10  $\mu$ L Trypan Blue dye (0.4%, Sigma-Aldrich) in a 1:1 ratio, and 10  $\mu$ L of the mixture was loaded onto a Neubauer hemocytometer for manual counting under a light microscope (Leica DM500).

Cell viability was calculated using the formula:

$$Viability (\%) = \frac{\text{Number of unstained cells}}{\text{Total number of cells}} \times 100$$

#### 4.6. Flow Cytometry for Apoptosis (Annexin V/PI Staining)

Apoptosis was assessed using Annexin V/ PI staining followed by flow cytometry to distinguish viable, early apoptotic, late apoptotic, and necrotic cells based on phosphatidylserine externalization and membrane integrity.

LNCaP cells were seeded in 6-well plates at  $2 \times 10^5$  cells per well in 2 mL of RPMI-1640 medium and allowed to adhere for 24 h at 37°C in a humidified incubator with 5% CO<sub>2</sub>. Cells were then treated with varying concentrations of *J. spicigera* extract, with 0.1% DMSO as the vehicle control and 10 µM etoposide (Sigma-Aldrich) as the positive control. Each condition was tested in three independent experiments.

Following treatment, cells were harvested by trypsinization (0.25% Trypsin-EDTA, Gibco) for 2 min at 37°C, neutralized with RPMI-1640 medium containing 10% FBS, and resuspended in cold PBS. A total of  $1 \times 10^5$  cells were transferred to fluorescence-activated cell sorting (FACS) tubes, centrifuged at  $300 \times g$  for 5 min, and resuspended in 100 µL of 1X Annexin V binding buffer (BD Biosciences). Cells were stained with 5 µL of Annexin V-FITC and 5 µL of propidium iodide (PI, 50 µg/mL, BD Biosciences) and incubated in the dark for 15 min at room temperature.

After incubation, 400 µL of 1X binding buffer was added, and samples were immediately analyzed using a flow cytometer (BD Accuri C6, BD Biosciences). Data was acquired from at least 10,000 events per sample, and analysis was performed using FlowJo v10 software (BD Biosciences).

Apoptotic cell populations were classified as: 1) annexin V<sup>-</sup>/PI<sup>-</sup> for viable cells; 2) annexin V<sup>+</sup>/PI<sup>-</sup> for early apoptotic cells; 3) annexin V<sup>+</sup>/PI<sup>+</sup> for late apoptotic cells; and 4) annexin V<sup>-</sup>/PI<sup>+</sup> for necrotic cells.

#### 4.6. Cell Cycle Analysis (PI Staining by Flow Cytometry)

To evaluate the effects of *J. spicigera* extract on cell cycle progression in LNCaP cells, PI staining followed by flow cytometry was performed. This method quantifies DNA content in individual cells, enabling the identification of G0/G1, S, and G2/M phases, as well as sub-G0/G1 populations indicative of apoptotic DNA fragmentation.

LNCaP cells were seeded at  $2 \times 10^5$  cells per well in 6-well plates containing 2 mL of RPMI-1640 medium and incubated at 37°C with 5% CO<sub>2</sub> for 24 h to allow adherence. Cells were then treated with varying concentrations of *J. spicigera* extract, with 0.1% DMSO as the vehicle control, 10 µM etoposide (Sigma-Aldrich) and 5-fluorouracil as the positive controls. Each condition was tested in three independent experiments.

Following treatment, both floating and adherent cells were collected by trypsinization (0.25% Trypsin-EDTA, Gibco) and centrifugation at  $300 \times g$  for 5 min at 4°C. The cell pellet was washed twice with cold phosphate-buffered saline (PBS, pH 7.4), resuspended in 500 µL of ice-cold PBS, and fixed by adding 1 mL of 70% ethanol dropwise while vortexing. Fixed cells were stored at -20°C for at least 24 h before further processing.

On the day of analysis, ethanol-fixed cells were centrifuged at  $500 \times g$  for 5 min, washed twice with PBS, and incubated with RNase A (100 µg/mL, Sigma-Aldrich) at 37°C for 30 min to eliminate RNA contamination. PI staining was performed by adding 50 µg/mL propidium iodide (Sigma-Aldrich) in PBS containing 0.1% Triton X-100, followed by incubation for 15 min in the dark at room temperature.

Flow cytometry analysis was conducted using a BD FACSCanto II flow cytometer (BD Biosciences), acquiring 10,000 events per sample on the FL2-A channel (PI fluorescence at 620 nm). The cell cycle distribution was analyzed using FlowJo v10 software (BD Biosciences) with the Watson pragmatic cell cycle modeling algorithm to determine the percentage of cells in G<sub>0</sub>/G<sub>1</sub>, S, and G<sub>2</sub>/M

phases. The sub-G<sub>0</sub>/G<sub>1</sub> population, indicative of apoptotic cells with fragmented DNA, was also quantified.

#### 4.7. Statistical Analysis

All experiments were performed in triplicate across three independent experiments, and data are presented as mean  $\pm$  standard error of the mean (SEM). Statistical significance was assessed using one-way ANOVA followed by Tukey's post hoc test, with  $p < 0.05$  and  $p < 0.001$ .

Flow cytometry data were analyzed using FlowJo v10 software (BD Biosciences), and cell cycle distribution was determined using the Watson pragmatic cell cycle modeling algorithm. All graphs and plots were generated using GraphPad Prism 10.0 (GraphPad Software, San Diego, CA, USA).

## 5. Conclusions

The hydroalcoholic extract of *Justicia spicigera* exhibited a clear dose-dependent antiproliferative effect on LNCaP prostate cancer cells, marked by G<sub>0</sub>/G<sub>1</sub> cell cycle arrest at 250  $\mu$ g/mL and apoptosis induction at concentrations  $\geq$ 500  $\mu$ g/mL. Flow cytometry confirmed inhibition of cell cycle progression, while Annexin V/PI staining revealed a shift toward apoptotic cell populations at higher doses. Phytochemical analysis identified kaempferitrin,  $\beta$ -sitosterol, and other flavonoids, compounds previously associated with regulation of p53, Bcl-2/Bax, and PI3K/Akt signaling pathways as likely contributors to these effects. The ability of the extract to curb proliferation without significant cytotoxicity at moderate concentrations suggests a therapeutic window that warrants further investigation. Evaluating its selectivity in non-malignant prostate epithelial cells and delineating its molecular targets will be critical next steps to assess its translational relevance. Additionally, its potential to synergize with existing therapies in both hormone-sensitive and castration-resistant prostate cancer models merits further exploration.

**Supplementary Materials:** The following supporting information can be downloaded at the website of this paper posted on Preprints.org, Figure S1. Thin-layer chromatography of *Justicia spicigera* extract; Figure S2. Thin-layer chromatography of the hydroalcoholic extract of *Justicia spicigera* of flavonoids; Figure S3. Thin-layer chromatography of the hydroalcoholic extract of *Justicia spicigera* of saponins; Figure S4. HPLC chromatogram of *Justicia spicigera* hydroalcoholic extract; Figure S5. LC-ESI-MS spectrum of *J. spicigera* extract; Figure S6. <sup>1</sup>H-NMR spectrum of the hydroalcoholic extract of *Justicia spicigera*.

**Author Contributions:** Conceptualization: T.J.P. F.R.R.-M, M.E.H.-A and M.G.-V.; Methodology: I.B-E and R.R.R.-H., E.C.-P; Software: I.B.-E. T.J.P.; Validation: T.J.P.; Formal analysis: I.B.-E, R.R.R.-H, C.A.L.-R. and S.G.-P.; Investigation: I.B.E., R.R.R.H. C.A.L.-R. and S.G.-P.; Resources: T.J.P. F.R.R.-M., M.G.-V, and F.H.-R.; Data curation: I.B.-E., R.R.R.H. and T.J.P.; Writing—original draft preparation: E.C.-P., C.A.L.-R., S.G.-P. and T.J.P.; Writing—review and editing: F.R.R.-M. and T.J.P.; Supervision: F.R.R.-M.; Project administration: F.R.R.-M. and T.J.P.; Funding acquisition: F.R.R.-M., T.J.P., M.G.-V, and F.H.-R.; All authors have read and agreed to the published version of the manuscript.

**Funding:** N/A

**Data Availability Statement:** The data produced from this study is available from the corresponding author upon reasonable request. This includes raw flow cytometry files, spectroscopic and chromatographic datasets, and processed quantitative analyses used in the evaluation of cell viability, apoptosis, and phytochemical composition.

**Acknowledgments:** I. B-E., C.A.R.-L. and S.G-P., thanks SECIHTI of Mexico for their Ph.D. scholarship [289304, 744624, and 792984 respectively]

**Conflicts of Interest:** The authors declare no conflicts of interest.

## References

1. Salud, S.d. Boletín epidemiológico. Sistema Nacional de Vigilancia Epidemiológica. Sistema Único de Información. Available online: <https://www.gob.mx/cms/uploads/attachment/file/967123/sem01.pdf> (accessed on 2nd june, 2025).
2. Instituto Nacional de Estadística, G.e.I. Defunciones registradas de hombres por tumor maligno de la próstata por entidad federativa de residencia habitual de la persona fallecida y grupo quinquenal de edad, serie anual de 2010 a 2023. Available online: [https://www.inegi.org.mx/app/tabulados/interactivos/?pxq=mortalidad\\_Mortalidad\\_06\\_d693a28d-07f6-4d7f-8d94-e7526498557b](https://www.inegi.org.mx/app/tabulados/interactivos/?pxq=mortalidad_Mortalidad_06_d693a28d-07f6-4d7f-8d94-e7526498557b) (accessed on 2nd june, 2025).
3. Ferlay, J.; Colombet, M.; Soerjomataram, I.; Parkin, D.M.; Pineros, M.; Znaor, A.; Bray, F. Cancer statistics for the year 2020: An overview. *Int J Cancer* **2021**, doi:10.1002/ijc.33588.
4. Sekhoacha, M.; Riet, K.; Motloung, P.; Gumenku, L.; Adegoke, A.; Mashele, S. Prostate Cancer Review: Genetics, Diagnosis, Treatment Options, and Alternative Approaches. *Molecules* **2022**, *27*, doi:10.3390/molecules27175730.
5. Lowrance, W.; Dreicer, R.; Jarrard, D.F.; Scarpato, K.R.; Kim, S.K.; Kirkby, E.; Buckley, D.I.; Griffin, J.C.; Cookson, M.S. Updates to Advanced Prostate Cancer: AUA/SUO Guideline (2023). *J Urol* **2023**, *209*, 1082-1090, doi:10.1097/JU.0000000000003452.
6. Sofi, F.A.; Tabassum, N. Natural product inspired leads in the discovery of anticancer agents: an update. *J Biomol Struct Dyn* **2023**, *41*, 8605-8628, doi:10.1080/07391102.2022.2134212.
7. Castro-Muñoz, R.; León-Becerril, E.; García-Depraet, O. Beyond the Exploration of Muicle (Justicia spicigera): Reviewing Its Biological Properties, Bioactive Molecules and Materials Chemistry. *Processes* **2022**, *10*, doi:10.3390/pr10051035.
8. Murillo-Villicana, M.; Noriega-Cisneros, R.; Pena-Montes, D.J.; Huerta-Cervantes, M.; Aguilera-Mendez, A.; Cortes-Rojo, C.; Salgado-Garciglia, R.; Montoya-Perez, R.; Riveros-Rosas, H.; Saavedra-Molina, A. Antilipidemic and Hepatoprotective Effects of Ethanol Extract of Justicia spicigera in Streptozotocin Diabetic Rats. *Nutrients* **2022**, *14*, doi:10.3390/nu14091946.
9. Rodriguez-Garza, N.E.; Quintanilla-Licea, R.; Romo-Saenz, C.I.; Elizondo-Luevano, J.H.; Tamez-Guerra, P.; Rodriguez-Padilla, C.; Gomez-Flores, R. In Vitro Biological Activity and Lymphoma Cell Growth Inhibition by Selected Mexican Medicinal Plants. *Life (Basel)* **2023**, *13*, doi:10.3390/life13040958.
10. Nan, Y.; Su, H.; Zhou, B.; Liu, S. The function of natural compounds in important anticancer mechanisms. *Front Oncol* **2022**, *12*, 1049888, doi:10.3389/fonc.2022.1049888.
11. Perez-Vasquez, A.; Diaz-Rojas, M.; Castillejos-Ramirez, E.V.; Perez-Esquivel, A.; Montano-Cruz, Y.; Rivero-Cruz, I.; Torres-Colin, R.; Gonzalez-Andrade, M.; Rodriguez-Sotres, R.; Gutierrez-Gonzalez, J.A.; et al. Protein tyrosine phosphatase 1B inhibitory activity of compounds from Justicia spicigera (Acanthaceae). *Phytochemistry* **2022**, *203*, 113410, doi:10.1016/j.phytochem.2022.113410.
12. Ortiz-Andrade, R.; Cabanas-Wuan, A.; Arana-Argaez, V.E.; Alonso-Castro, A.J.; Zapata-Bustos, R.; Salazar-Olivo, L.A.; Dominguez, F.; Chavez, M.; Carranza-Alvarez, C.; Garcia-Carranca, A. Antidiabetic effects of Justicia spicigera Schleidl (Acanthaceae). *J Ethnopharmacol* **2012**, *143*, 455-462, doi:10.1016/j.jep.2012.06.043.
13. Angeles-Lopez, G.E.; Gonzalez-Trujano, M.E.; Rodriguez, R.; Deciga-Campos, M.; Brindis, F.; Ventura-Martinez, R. Gastrointestinal activity of Justicia spicigera Schleidl. in experimental models. *Nat Prod Res* **2021**, *35*, 1847-1851, doi:10.1080/14786419.2019.1637873.
14. Carneiro, M.R.B.; Sallum, L.O.; Martins, J.L.R.; Peixoto, J.C.; Napolitano, H.B.; Rosseto, L.P. Overview of the Justicia Genus: Insights into Its Chemical Diversity and Biological Potential. *Molecules* **2023**, *28*, doi:10.3390/molecules28031190.
15. De La Cruz-Jimenez, L.; Hernandez-Torres, M.A.; Monroy-Garcia, I.N.; Rivas-Morales, C.; Verde-Star, M.J.; Gonzalez-Villasana, V.; Viveros-Valdez, E. Biological Activities of Seven Medicinal Plants Used in Chiapas, Mexico. *Plants (Basel)* **2022**, *11*, doi:10.3390/plants11141790.
16. Euler, K.L.; Alam, M. Isolation of Kaempferitrin From Justicia spicigera. *Journal of Natural Products* **1982**, *45*, 220-221, doi:10.1021/np50020a020.
17. Dominguez XA, A.H., González C, Ferreé -D'Amare AR. Estudio químico del "muitle" (Justicia spicigera). *Rev Latinoamer Quím* **1990**, *21*, 142-143.

18. Zapata-Morales, J.R.; Alonso-Castro, A.J.; Gonzalez-Rivera, M.L.; Gonzalez Prado, H.I.; Barragan-Galvez, J.C.; Hernandez-Flores, A.; Juarez-Vazquez, M.D.C.; Dominguez, F.; Carranza-Alvarez, C.; de Jesus Pozos-Guillen, A.; et al. Synergistic Interaction Between *Justicia spicigera* Extract and Analgesics on the Formalin Test in Rats. *Pharmaceuticals (Basel)* **2025**, *18*, doi:10.3390/ph18020187.
19. Arberet, L.; Pottier, F.; Michelin, A.; Nowik, W.; Bellot-Gurlet, L.; Andraud, C. Spectral characterisation of a traditional Mesoamerican dye: relationship between in situ identification on the 16(th) century Codex Borbonicus manuscript and composition of *Justicia spicigera* plant extract. *Analyst* **2021**, *146*, 2520-2530, doi:10.1039/d1an00113b.
20. Awad, N.E.; Abdelkawy, M.A.; Abdel Rahman, E.H.; Hamed, M.A.; Ramadan, N.S. Phytochemical and in vitro Screening of *Justicia spicigera* Ethanol Extract for Antioxidant Activity and in vivo Assessment Against *Schistosoma mansoni* Infection in Mice. *Anti-Infective Agents* **2018**, *16*, 49-56, doi:10.2174/2211352516666180126161247.
21. Shahzad, N.; Khan, W.; Md, S.; Ali, A.; Saluja, S.S.; Sharma, S.; Al-Allaf, F.A.; Abduljaleel, Z.; Ibrahim, I.A.A.; Abdel-Wahab, A.F.; et al. Phytosterols as a natural anticancer agent: Current status and future perspective. *Biomed Pharmacother* **2017**, *88*, 786-794, doi:10.1016/j.bioph.2017.01.068.
22. Caceres-Cortes, J.R.; Cantu-Garza, F.A.; Mendoza-Mata, M.T.; Chavez-Gonzalez, M.A.; Ramos-Mandujano, G.; Zambrano-Ramirez, I.R. Cytotoxic activity of *Justicia spicigera* is inhibited by bcl-2 proto-oncogene and induces apoptosis in a cell cycle dependent fashion. *Phytother Res* **2001**, *15*, 691-697, doi:10.1002/ptr.791.
23. Vega-Avila, E.; Tapia-Aguilar, Rafaela; Reyes-Chilpa, Ricardo; Guzmán-Gutiérrez, Silvia Laura; Pérez-Flores, Javier, & Velasco-Lezama, Rodolfo. Actividad antibacteriana y antifúngica de *Justicia Spicigera*. *Rev. latinoam. quím* **2012**, *40*, 75-82.
24. Jacobo-Salcedo, M.d.R.; Alonso-Castro, A.J.; Salazar-Olivo, L.A.; Carranza-Alvarez, C.; González-Espíndola, L.Á.; Domínguez, F.; Maciel-Torres, S.P.; García-Lujan, C.; González-Martínez, M.d.R.; Gómez-Sánchez, M.; et al. Antimicrobial and Cytotoxic Effects of Mexican Medicinal Plants. *Natural Product Communications* **2011**, *6*, doi:10.1177/1934578x1100601234.
25. Del Carmen Juarez-Vazquez, M.; Josabad Alonso-Castro, A.; Garcia-Carranca, A. Kaempferitrin induces immunostimulatory effects in vitro. *J Ethnopharmacol* **2013**, *148*, 337-340, doi:10.1016/j.jep.2013.03.072.
26. Fernández-Pomares, C.; Juárez-Aguilar, E.; Domínguez-Ortiz, M.Á.; Gallegos-Estudillo, J.; Herrera-Covarrubias, D.; Sánchez-Medina, A.; Aranda-Abreu, G.E.; Manzo, J.; Hernández, M.E. Hydroalcoholic extract of the widely used Mexican plant *Justicia spicigera* Schltdl. exerts a cytostatic effect on LNCaP prostate cancer cells. *Journal of Herbal Medicine* **2018**, *12*, 66-72, doi:10.1016/j.hermed.2017.09.003.
27. Real-Sandoval, S.A.; Gutiérrez-López, G.F.; Domínguez-López, A.; Paniagua-Castro, N.; Michicotl-Meneses, M.M.; Jaramillo-Flores, M.E. Downregulation of proinflammatory liver gene expression by *Justicia spicigera* and kaempferitrin in a murine model of obesity-induced by a high-fat diet. *Journal of Functional Foods* **2020**, *65*, doi:10.1016/j.jff.2020.103781.
28. Kopustinskiene, D.M.; Jakstas, V.; Savickas, A.; Bernatoniene, J. Flavonoids as Anticancer Agents. *Nutrients* **2020**, *12*, doi:10.3390/nu12020457.
29. Jia, X.B.; Zhang, Q.; Xu, L.; Yao, W.J.; Wei, L. Lotus leaf flavonoids induce apoptosis of human lung cancer A549 cells through the ROS/p38 MAPK pathway. *Biol Res* **2021**, *54*, 7, doi:10.1186/s40659-021-00330-w.
30. Jomova, K.; Alomar, S.Y.; Valko, R.; Liska, J.; Nepovimova, E.; Kuca, K.; Valko, M. Flavonoids and their role in oxidative stress, inflammation, and human diseases. *Chem Biol Interact* **2025**, *413*, doi:10.1016/j.cbi.2025.111489.
31. Rahman, N.; Khan, H.; Zia, A.; Khan, A.; Fakhri, S.; Aschner, M.; Gul, K.; Saso, L. Bcl-2 Modulation in p53 Signaling Pathway by Flavonoids: A Potential Strategy towards the Treatment of Cancer. *Int J Mol Sci* **2021**, *22*, doi:10.3390/ijms22111315.
32. Wong, S.C.; Kamarudin, M.N.A.; Naidu, R. Anticancer Mechanism of Flavonoids on High-Grade Adult-Type Diffuse Gliomas. *Nutrients* **2023**, *15*, doi:10.3390/nu15040797.
33. Zhou, S.; Zhang, H.; Li, J.; Li, W.; Su, M.; Ren, Y.; Ge, F.; Zhang, H.; Shang, H. Potential anti-liver cancer targets and mechanisms of kaempferitrin based on network pharmacology, molecular docking and experimental verification. *Comput Biol Med* **2024**, *178*, 108693, doi:10.1016/j.combiomed.2024.108693.

34. Su, M.; Li, Z.; Zhou, S.; Zhang, H.; Xiao, Y.; Li, W.; Shang, H.; Li, J. Kaempferitrin, a major compound from ethanol extract of *Chenopodium ambrosioides*, exerts antitumour and hepatoprotective effects in the mice model of human liver cancer xenografts. *J Pharm Pharmacol* **2023**, *75*, 1066-1075, doi:10.1093/jpp/rgad046.
35. Zhu, X.; Pan, Y.; Xu, X.; Xu, J. Kaempferitrin alleviates LPS-induced septic acute lung injury in mice through downregulating NF-kappaB pathway. *Allergol Immunopathol (Madr)* **2023**, *51*, 1-7, doi:10.15586/aei.v51i6.838.
36. Shi, Z.; Shen, Y.; Liu, X.; Zhang, S. Kaempferitrin Regulates the Proliferation, Metastasis, and Immune Escape of Nonsmall Cell Lung Cancer by Inhibiting the Akt/NF-kappaB Pathway. *Drug Dev Res* **2025**, *86*, e70117, doi:10.1002/ddr.70117.
37. Chen, Y.; He, S.; Zeng, A.; He, S.; Jin, X.; Li, C.; Mei, W.; Lu, Q. Inhibitory Effect of beta-Sitosterol on the Ang II-Induced Proliferation of A7r5 Aortic Smooth Muscle Cells. *Anal Cell Pathol (Amst)* **2023**, *2023*, 2677020, doi:10.1155/2023/2677020.
38. Lin, F.; Xu, L.; Huang, M.; Deng, B.; Zhang, W.; Zeng, Z.; Yinzhi, S. beta-Sitosterol Protects against Myocardial Ischemia/Reperfusion Injury via Targeting PPARgamma/NF-kappaB Signalling. *Evid Based Complement Alternat Med* **2020**, *2020*, 2679409, doi:10.1155/2020/2679409.
39. Elasbali, A.M.; Al-Soud, W.A.; Al-Oanzi, Z.H.; Qanash, H.; Alharbi, B.; Binsaleh, N.K.; Alreshidi, M.; Patel, M.; Adnan, M. Cytotoxic Activity, Cell Cycle Inhibition, and Apoptosis-Inducing Potential of *Athyrium hohenackerianum* (Lady Fern) with Its Phytochemical Profiling. *Evid Based Complement Alternat Med* **2022**, *2022*, 2055773, doi:10.1155/2022/2055773.
40. Pilling, A.; Kim, S.H.; Hwang, C. Androgen receptor negatively regulates mitotic checkpoint signaling to induce docetaxel resistance in castration-resistant prostate cancer. *Prostate* **2022**, *82*, 182-192, doi:10.1002/pros.24257.
41. Alonso-Castro, A.J.; Ortiz-Sanchez, E.; Garcia-Regalado, A.; Ruiz, G.; Nunez-Martinez, J.M.; Gonzalez-Sanchez, I.; Quintanar-Jurado, V.; Morales-Sanchez, E.; Dominguez, F.; Lopez-Toledo, G.; et al. Kaempferitrin induces apoptosis via intrinsic pathway in HeLa cells and exerts antitumor effects. *J Ethnopharmacol* **2013**, *145*, 476-489, doi:10.1016/j.jep.2012.11.016.

**Disclaimer/Publisher's Note:** The statements, opinions and data contained in all publications are solely those of the individual author(s) and contributor(s) and not of MDPI and/or the editor(s). MDPI and/or the editor(s) disclaim responsibility for any injury to people or property resulting from any ideas, methods, instructions or products referred to in the content.